bioRxiv preprint doi: https://doi.org/10.1101/362079; this version posted July 4, 2018. The copyright holder for this preprint (which was not certified by peer review) is the author/funder, who has granted bioRxiv a license to display the preprint in perpetuity. It is made available under aCC-BY-NC-ND 4.0 International license.

1 **Gorilla APOBEC3 restricts SIVcpz and influences lentiviral evolution in great**
2 **ape cross-species transmissions**
3
4 Yusuke Nakano[1], Keisuke Yamamoto[1,2], Andrew Soper[1,2], Ryuichi Kumata[1,3],
5 Hirofumi Aso[1,4], Naoko Misawa[1], Yoriyuki Konno[1,5], Izumi Kimura[1,4], Shumpei
6 Nagaoka[1,5], Guillermo Juarez-Fernandez[1,2], Jumpei Ito[1], Terumasa Ikeda[6-10],
7 Yoshio Koyanagi[1], Reuben S Harris[6-10] and Kei Sato[1,11,12,13]*
8
9 [1]Laboratory of Systems Virology, Institute for Frontier Life and Medical Sciences,
10 [2]Graduate School of Medicine,
11 [3]Faculty of Science,
12 [4]Graduate School of Pharmaceutical Sciences,
13 [5]Graduate School of Biostudies,
14 Kyoto University, Kyoto 6068507, Japan.
15 [6]Department of Biochemistry, Molecular Biology and Biophysics,
16 [7]Masonic Cancer Center,
17 [8]Institute for Molecular Virology,
18 [9]Center for Genome Engineering,
19 University of Minnesota, Minneapolis, Minnesota 55455, USA.
20 [10]Howard Hughes Medical Institute, University of Minnesota, Minneapolis,
21 Minnesota 55455, USA.
22 [11]CREST, Japan Science and Technology Agency, Saitama 3220012, Japan.
23 [12]Division of Systems Virology, Department of Infectious Disease Control,
24 International Research Center for Infectious Diseases, Institute of Medical Science,
25 The University of Tokyo, Tokyo 1088639, Japan.
26 [13]Lead Contact
27 *Correspondence: ksato@ims.u-tokyo.ac.jp (K.S.)
28
29 **Conflict of interest**: The authors declare that no competing interests exist.
30 **Keywords**: HIV; SIV; Vif; APOBEC3; viral evolution; cross-species transmission
31
32 140/150 words in Summary; 37,930/38,000 characters in text

bioRxiv preprint doi: https://doi.org/10.1101/362079; this version posted July 4, 2018. The copyright holder for this preprint (which was not certified by peer review) is the author/funder, who has granted bioRxiv a license to display the preprint in perpetuity. It is made available under aCC-BY-NC-ND 4.0 International license.

33 **Highlights**

34 - SIVcpz requires M16E mutation in Vif to counteract gorilla A3G
35 - Acidic residue at position 16 of Vif is crucial to counteract gorilla A3G
36 - Gorilla A3D and A3F poorly suppress lentiviral infectivity
37 - SIVgor and related HIV-1s counteract human A3D and A3F independently of
38 DRMR motif

39
40

41 **Summary**

42 Restriction factors including APOBEC3 family proteins have the potential prevent
43 cross-species lentivirus transmissions. Such events as well as ensuing
44 pathogenesis require the viral Vif protein to overcome/neutralize/degrade the
45 APOBEC3 enzymes of the new host species. Previous investigations have focused
46 on the molecular interaction between human APOBEC3s and HIV-1 Vif. However,
47 the evolutionary interplay between lentiviruses and great ape (including human,
48 chimpanzee and gorilla) APOBEC3s has not been fully investigated. Here we
49 demonstrate that gorilla APOBEC3G plays a pivotal role in restricting lentiviral
50 transmission from chimpanzee to gorilla. We also reveal that a sole amino acid
51 substitution in Vif is sufficient to overcome the gorilla APOBEC3G-mediated species
52 barrier. Moreover, the antiviral effects of gorilla APOBEC3D and APOBEC3F are
53 considerably weaker than those of human and chimpanzee counterparts, which can
54 result in the skewed evolution of great ape lentiviruses leading to HIV-1.

bioRxiv preprint doi: https://doi.org/10.1101/362079; this version posted July 4, 2018. The copyright holder for this preprint (which was not certified by peer review) is the author/funder, who has granted bioRxiv a license to display the preprint in perpetuity. It is made available under aCC-BY-NC-ND 4.0 International license.

55 **Introduction**

56 Lentiviruses were identified in great apes including humans (*Homo*
57 *sapiens*; HU), central chimpanzees (*Pan troglodytes troglodytes*; CPZ), eastern
58 chimpanzees (*Pan troglodytes schweinfurthii*), and gorillas (*Gorilla gorilla gorilla*;
59 GOR). The lentiviruses isolated from their respective hosts were designated HIV
60 (Barre-Sinoussi et al., 1983), SIVcpz*Ptt* [simian immunodeficiency virus (SIV) in
61 CPZ] (Gao et al., 1999; Keele et al., 2006), SIVcpz*Pts* (SIV in eastern chimpanzee)
62 (Vanden Haesevelde et al., 1996), and SIVgor (SIV in GOR) (Van Heuverswyn et
63 al., 2006). HIV type 1 (HIV-1) is classified into four groups, M (major), N
64 (non-M-non-O), O (outlier) and P (reviewed in (Sharp and Hahn, 2011). Molecular
65 phylogenetic analyses indicate that that HIV-1M and HIV-1N originated from
66 SIVcpz*Ptt* (Keele et al., 2006), while HIV-1O and HIV-1P are derived from SIVgor
67 (D'arc et al., 2015). These insights indicate that HIV-1s emerged by cross-species
68 viral transmission from CPZ and GOR, respectively.
69
70 To potently control cross-species lentiviral transmission, several cellular
71 restriction factors such as TRIM5, tetherin, SAMHD1 and APOBEC3 (A3) proteins
72 were identified [reviewed in (Doyle et al., 2015; Kluge et al., 2015)]. One of the
73 well-studied restriction factors that potently restricts cross-species transmission of
74 great ape lentiviruses is HU tetherin. To overcome the HU tetherin-mediated
75 antiviral effect, the viral protein U (Vpu) of HIV-1M, a pandemic virus group,
76 down-modulates and antagonizes HU tetherin (Neil et al., 2008; Van Damme et al.,
77 2008). Since the Vpu protein of SIVcpz*Ptt*, the ancestral virus of HIV-1M (Keele et
78 al., 2006), is incapable of counteracting HU tetherin (Sauter et al., 2009), these
79 observations imply that HU tetherin functions as barrier restricting cross-species
80 lentiviral transmission from CPZ to HU, and that acquiring anti-HU tetherin activity is
81 essential for the successful cross-species jump [reviewed in (Kirchhoff, 2010)].
82
83 Another group of well-understood restriction factors is the A3 DNA
84 deaminase family. Most great apes encode seven A3 proteins [reviewed in (Nakano
85 et al., 2017a)]. At least three, A3D, A3F, and A3G, are packaged into nascent viral
86 particles and suppress viral infectivity through inserting G-to-A mutations in the viral
87 genome [reviewed in (Harris and Dudley, 2015)]. To counteract A3-mediated
88 restriction action, viral infectivity factor (Vif), an accessory protein of lentiviruses,
89 recruits cellular E3 ubiquitin ligase complex and degrades the host A3 proteins via a
90 ubiquitin-proteasome-dependent pathway [reviewed in (Harris and Dudley, 2015)].
91 Because Vif-mediated counteraction of antiviral A3 is largely species-specific, it is
92 suggested that lentiviral *vif* and mammalian *A3* genes have co-evolve [reviewed in

bioRxiv preprint doi: https://doi.org/10.1101/362079; this version posted July 4, 2018. The copyright holder for this preprint (which was not certified by peer review) is the author/funder, who has granted bioRxiv a license to display the preprint in perpetuity. It is made available under aCC-BY-NC-ND 4.0 International license.

93 (Nakano et al., 2017a)]. For instance, it has been reported that Old world monkey
94 A3G proteins contribute to restrict lentiviral transmission among these species
95 (Compton et al., 2014; Compton and Emerman, 2013).
96
97 SIVgor was first discovered from the fecal samples of wild GORs, which
98 were obtained in remote forest regions in Cameroon in 2007 (Van Heuverswyn et
99 al., 2006). A following study revealed that SIVgor is phylogenetically related to
100 HIV-1 groups O and P (D'arc et al., 2015), suggesting that SIVgor is the ancestral
101 virus of these HIV-1s in the human population. Moreover, a phylogenetic analysis
102 deduced that SIVgor emerged from the leap of SIVcpz*Ptt* from CPZ to GOR
103 (Takehisa et al., 2009).
104
105 The molecular interactions between HIV-1 Vif and HU A3 proteins are well
106 established [reviewed in (Harris and Dudley, 2015)]. Also, the functional and
107 evolutionary relationships between SIVcpz*Ptt* Vif and HU A3 proteins have been
108 investigated (Letko et al., 2013; Sato et al., 2018; Zhang et al., 2017). However, the
109 evolutionary episodes of great ape lentiviruses through GOR, namely, the
110 emergence of (i) SIVgor from SIVcpz*Ptt*; and (ii) HIV-1OP from SIVgor, have not
111 been fully investigated. Moreover, the functional and evolutionary association of
112 great ape lentiviral Vif with their host A3 proteins remains unclear. In this study, we
113 focus on the antiviral effects of great ape A3 proteins including GOR A3s and their
114 antagonistic mechanisms by great ape lentiviral Vif proteins. To the best of our
115 knowledge, this is the first report suggesting that a great ape A3 protein potently
116 restricts the cross-species leap of great ape lentiviruses and illustrates the
117 evolutionary scenario of great ape lentiviruses via the interaction of great ape A3
118 proteins.

bioRxiv preprint doi: https://doi.org/10.1101/362079; this version posted July 4, 2018. The copyright holder for this preprint (which was not certified by peer review) is the author/funder, who has granted bioRxiv a license to display the preprint in perpetuity. It is made available under aCC-BY-NC-ND 4.0 International license.

119 **Results**

120 **GOR A3G restricts SIVcpz*Ptt* infection**

121 **Figure 1A** illustrates a phylogenetic tree of *vif* genes of great ape
122 lentiviruses. This phylogenetic tree indicates that HIV-1M and HIV-1N form clusters
123 with SIVcpz*Ptt*, while HIV-1O and HIV-1P are together with SIVgor. Consistent with
124 previous reports, it is suggested that HIV-1M and HIV-1N originated from SIVcpz*Ptt*
125 (Keele et al., 2006), while HIV-1O and HIV-1P are derived from SIVgor (D'arc et al.,
126 2015) (**Figure 1B**).

127 To address the possibility that great ape A3G can be a factor restricting
128 cross-species transmission of great ape lentiviruses, we set out to analyze the
129 antiviral activity of great ape A3G. We co-transfected the expression plasmids of
130 great ape (HU, CPZ and GOR) A3G with an infectious molecular clone (IMC) of
131 *vif*-deleted HIV-1. All great ape A3Gs exhibited comparably strong and
132 dose-dependent antiviral effects (**Figure S1B and S1C**).

133 To assess the ability of lentiviral Vif to counteract host A3G, the expression
134 plasmid for HU A3G was co-transfected together with the Vif expression plasmids
135 and an IMC of *vif*-deleted HIV-1. As shown in **Figure 1C**, all lentiviral Vifs including
136 HIV-1MNOP, SIVcpz*Ptt* and SIVgor degraded HU A3G and impaired the
137 incorporation of HU A3G into the released virions. Also, in the presence of HU A3G,
138 the viral infectivity was rescued by all lentiviral Vifs tested in this study (**Figure 1D**).
139 These findings suggest that HU A3G does not restrict cross-species transmission of
140 SIVs from CPZ and GOR to HU. In sharp contrast, we found that GOR A3G was
141 antagonized by SIVgor Vif but not by SIVcpz*Ptt* Vif (**Figures 1E and 1F**). These
142 findings strongly suggested that the antiviral activity of GOR A3G had to be
143 overcome for cross-species transmission of SIVcpz*Ptt* from CPZ to GOR.

144

145 **M16E mutation confers anti-GOR A3G ability on SIVcpz*Ptt* Vif**

146 To investigate how SIVgor acquired the ability to counteract GOR A3G, we
147 next performed gain-of-function experiments based on SIVcpz*Ptt* Vif (strain MB897).
148 We first prepared four chimeric Vif mutants of SIVcpz*Ptt* MB897 and SIVgor
149 CP2139 (chimeras A-D; **Figure 2A**) and evaluated their ability to counteract GOR
150 A3G-mediated antiviral action using the cell-based single-round infection assays.
151 As shown in **Figure 2B**, SIVgor CP2139 Vif as well as chimera A Vif overcame the

bioRxiv preprint doi: https://doi.org/10.1101/362079; this version posted July 4, 2018. The copyright holder for this preprint (which was not certified by peer review) is the author/funder, who has granted bioRxiv a license to display the preprint in perpetuity. It is made available under aCC-BY-NC-ND 4.0 International license.

152 GOR A3G-mediated antiviral effect, suggesting that the N-terminal domain of
153 SIVgor is responsible for the counteraction of GOR A3G. We then prepared five
154 additional mutants (chimeras A1-A5) and performed cell-based co-transfection
155 experiments. We found that only chimera A1 is able to degrade GOR A3G (**Figure**
156 **2C, top**) and therefore rescues the infectivity of released viruses (**Figure 2C,**
157 **bottom**). Only three amino acid differences occur in this region (**Figure S2A**).
158 Individual mutants were analyzed and only M16E, not the K6Q or D14P, conferred
159 the ability to counteract GOR A3G (**Figure 2D**). To analyze the effect of M16E
160 mutation on viral spread, we constructed the mutant IMCs of SIVcpz*Ptt* MB897 and
161 prepared the viral supernatant. The infectivity of the M16E and E2X (*vif*-deleted)
162 variants was comparable to wild-type (WT) virus in the absence of A3s (**Figure**
163 **S2B**). We inoculated these viruses into the HU A3-null SupT11-CCR5 cells and the
164 SupT11-CCR5 cells stably expressing GOR A3G (SupT11-CCR5-GOR A3G)
165 (**Figure S2C**). In parental SupT11-CCR5 cells, these three viruses replicated
166 similarly (**Figure 2E, left**). On the other hand, in SupT11-CCR5-GOR A3G cells, the
167 growth kinetics of the M16E mutant was significantly higher than those of WT and
168 the E2X mutant (**Figure 2E, right**). Moreover, with regard to the area under the
169 curve indicating the amount of cumulative viruses released in the culture
170 supernatant, this value of the M16E mutant was significantly higher than those of
171 WT and the E2X mutant in SupT11-CCR5-GOR A3G cells (**Figure 2F**). These
172 findings show that Vif position 16 is an important determinant of GOR A3G
173 counteraction.

174 As shown in **Figure S2D**, M16 in Vif is conserved among 16 different
175 SIVcpz*Ptt* strains. To ask whether the substitution of methionine to glutamic acid
176 broadly contributes to the gain-of-function of SIVcpz*Ptt* Vif to counteract GOR A3G,
177 we constructed M16E mutants of additional SIVcpz*Ptt* strains, CAM3, DP943,
178 MT145 and LB7. Although the WT Vifs of these SIVcpz*Ptt* strains were unable to
179 counteract GOR A3G, all M16E mutants of SIVcpz*Ptt* Vif tested in this experiment
180 acquired the ability to counteract GOR A3G (**Figure 2G**). These findings suggest
181 that the acquisition of anti-GOR A3G ability by the M16E substitution is not specific
182 for SIVcpz*Ptt* strain MB897 but shared among SIVcpz*Ptt* strains.

183 We next assessed the side-chain properties of position 16 of SIVcpz*Ptt* Vif
184 to counteract GOR A3G. To address this, we constructed three additional mutants

bioRxiv preprint doi: https://doi.org/10.1101/362079; this version posted July 4, 2018. The copyright holder for this preprint (which was not certified by peer review) is the author/funder, who has granted bioRxiv a license to display the preprint in perpetuity. It is made available under aCC-BY-NC-ND 4.0 International license.

185 at position 16. In addition to the M16E mutant, the M16D mutant of MB897 Vif
186 counteracted the GOR A3G-mediated antiviral effect, while the M16A and M16Q
187 mutants did not (**Figure 2H**). Taken together, these results suggested that acquiring
188 an acidic residue at position 16 is sufficient to counteract GOR A3G-mediated
189 antiviral effect.
190

191 **GOR A3D and A3F poorly exhibit antiviral effect**

192 It is known that the DRMR motif, residues positioned between 14-17 in Vif,
193 are crucial to counteract HU A3D and A3F (Russell et al., 2009; Sato et al., 2014).
194 Since M16E is located in this motif, we next investigated the association of GOR
195 A3D and A3F with great ape lentiviruses. We co-transfected the expression
196 plasmids of great ape A3D or A3F with an IMC of *vif*-deleted HIV-1. Interestingly,
197 the expression levels of GOR A3D (**Figure 3A, top**) and A3F (**Figure 3C, top**) were
198 clearly lower than those of HU and CPZ counterparts. Also, the amounts of GOR
199 A3D (**Figure 3A, bottom**) and A3F (**Figure 3C, bottom**) in the released viral
200 particles as well as the antiviral effects of GOR A3D (**Figure 3B**) and A3F (**Figure**
201 **3D**) were lower than those of HU and CPZ counterparts. These data suggest that
202 GOR A3D and A3F are poorly expressed and faintly exhibit antiviral effect when
203 compared to HU and CPZ counterparts.
204

205 **Vif DRMR motif is distortedly evolved in GOR**

206 We next assessed the conservation of the DRMR motif in great ape
207 lentiviral Vif. As shown in **Figure 4A**, this motif is highly conserved in HIV-1M,
208 HIV-1N, SIVcpz*Ptt* and SIVcpz*Pts*, another group of SIVcpz in a subspecies of
209 chimpanzee (eastern chimpanzee; *Pan troglodytes schweinfurthii*). In contrast, this
210 domain is altered in HIV-1O, HIV-1P and SIVgor (**Figure 4A**). Moreover, the
211 molecular phylogenetic analysis on the Vif DRMR motif indicated that this motif in
212 HIV-1O, HIV-1P and SIVgor forms separated clusters to HIV-1M, HIV-1N,
213 SIVcpz*Ptt* and SIVcpz*Pts* with higher bootstrap values (**Figure S3A**). Since the
214 YRHHY motif positioned between 40-44 in Vif, which is responsible for A3G
215 counteraction (Russell et al., 2009; Sato et al., 2014), is highly conserved in all
216 great ape lentiviruses (**Figure 4A**), these findings suggest that the Vif DRMR motif
217 may be less functionally constrained.

bioRxiv preprint doi: https://doi.org/10.1101/362079; this version posted July 4, 2018. The copyright holder for this preprint (which was not certified by peer review) is the author/funder, who has granted bioRxiv a license to display the preprint in perpetuity. It is made available under aCC-BY-NC-ND 4.0 International license.

218 The loss of the DRMR motif in the Vifs of HIV-1O, HIV-1P and SIVgor
219 raised the possibility that these Vifs are unable to counteract A3D and A3F from HU
220 and GOR. To address this issue, the expression plasmids for HU A3D or A3F were
221 co-transfected together with the Vif expression plasmids and an IMC of *vif*-deleted
222 HIV-1. As shown in **Figures 4B and 4C**, it was surprising that the all Vifs tested
223 including those from HIV-1O, HIV-1P and SIVgor counteracted both HU A3D and
224 A3F. These Vifs also counteracted GOR A3D and A3F (**Figure S3B and S3C**).
225 These findings (**Figures 4A-4C**) suggested that Vif amino acids 14-17 in
226 HIV-1O, HIV-1P and SIVgor may be dispensable for counteracting HU A3D and
227 A3F. To address this possibility, we constructed chimeric mutants of HIV-1M strain
228 JRCSF Vif that possess the amino acid residues of HIV-1O, HIV-1P and SIVgor at
229 the corresponding positions: DRQK (from HIV-1O), SREK (from HIV-1P), PREK
230 (from HIV-1P) and PRER (from SIVgor) (**Figure 4D**). Although the Vifs of HIV-1O,
231 HIV-1P and SIVgor successfully counteracted HU A3D and A3F (**Figures 4B and**
232 **4C**), the JRCSF Vif mutants possessing the amino acid residues of HIV-1O (DRQK),
233 HIV-1P (SREK and PREK) and SIVgor (PRER) instead of DRMR were unable to
234 counteract HU A3D (**Figure 4E**) and A3F (**Figure 4F**). Taken together, these
235 findings suggest that HIV-1O, HIV-1P and SIVgor overcome the antiviral effects
236 mediated by A3D and A3F of HU and GOR independently of the Vif DRMR motif.

bioRxiv preprint doi: https://doi.org/10.1101/362079; this version posted July 4, 2018. The copyright holder for this preprint (which was not certified by peer review) is the author/funder, who has granted bioRxiv a license to display the preprint in perpetuity. It is made available under aCC-BY-NC-ND 4.0 International license.

237 **Discussion**

238 In the present study, we demonstrated that HU A3D, A3F, and A3G are
239 counteracted by all great ape lentiviral Vifs tested in this study. Our results are
240 consistent with previous observations that SIVcpz (Bibollet-Ruche et al., 2012) and
241 SIVgor (Takehisa et al., 2009) are able to replicate in *in vitro* human CD4$^+$ T-cell
242 culture. Moreover, SIVcpz efficiently expands in a hematopoietic stem
243 cell-transplanted humanized mouse model (Sato et al., 2018; Yamada et al., 2018).
244 Taken together with our findings, these observations suggest that HU A3 proteins
245 may not have been a barrier to SIV transmission from CPZ and GOR to HU. In
246 contrast, SIVcpz*Ptt* Vif was incapable of antagonizing the GOR A3G-mediated
247 antiviral effect. Here we demonstrated that an amino acid substitution at position 16
248 of SIVcpz*Ptt* Vif is sufficient to acquire the ability to counteract GOR A3G. Our
249 findings suggest that GOR A3G restriction activity had to be overcome for
250 transmission from of SIVcpz*Ptt* from CPZ to GOR. To the best of our knowledge,
251 this is the first report providing evidence that a great ape A3 protein plays a crucial
252 role in restricting the leap of great ape lentivirus between different host species and
253 how exactly primate lentiviruses overcame the hurdle mediated by host antiviral A3
254 protein. Furthermore, we revealed that the antiviral effects of GOR A3D and A3F
255 are relatively weaker than those of HU and CPZ counterparts and that the Vif
256 DRMR motif, which is important to counteract HU A3D and A3F (Russell et al.,
257 2009; Sato et al., 2014), has been lost in SIVgor and related HIV-1s (groups O and
258 P). These findings suggest that the evolutionary process of great ape lentiviruses
259 leading to HIV-1 in HU was uniquely skewed via SIV infection in GOR.

260

261 With regard to the functional interaction between GOR A3G and the Vif
262 proteins of SIVcpz*Ptt* and SIVgor, a previous paper revealed that the amino acid
263 positioned at 129 of GOR A3G determines the sensitivity to SIVgor Vif-mediated
264 degradation (D'arc et al., 2015). Interestingly, only GOR A3G possesses glutamine
265 at position 129 while the A3G of other primates including HU and CPZ possesses
266 proline at that position (Letko et al., 2015; Letko et al., 2013). However, because of
267 the low sequence similarity on the *vif* genes of SIVcpz*Ptt* and SIVgor (69.6%
268 nucleotide sequence similarity between SIVcpz*Ptt* strain MB897 and SIVgor strain
269 CP2139, both of which were used in this study for chimeric Vif preparation [**Figure**

bioRxiv preprint doi: https://doi.org/10.1101/362079; this version posted July 4, 2018. The copyright holder for this preprint (which was not certified by peer review) is the author/funder, who has granted bioRxiv a license to display the preprint in perpetuity. It is made available under aCC-BY-NC-ND 4.0 International license.

270 **2A**]; p-distance between SIVcpz*Ptt* *vif* and SIVgor *vif* = 0.373 ± 0.013), the
271 responsible residue(s) in Vif determining the ability to counteract GOR A3G were
272 not revealed. Here we demonstrated that the ability of SIVcpz*Ptt* Vif to counteract
273 GOR A3G is acquired by a single amino acid substitution at the position 16.
274 Interestingly, with regard to the structural interaction between Vif and A3G, Letko et
275 al. have recently provided a co-structure model of Vif and A3G suggesting that the
276 amino acid residues located between 14-17 of Vif structurally interacts with the
277 residues located between 125-130 of A3G and that the electric charge of the
278 surface of respective domains on each protein associates with Vif-A3G interaction
279 (Letko et al., 2015). Taken together with our finding that the acquisition of an acidic
280 residue (glutamic acid or aspartic acid) at position 16 of SIVcpz*Ptt* Vif confers the
281 ability to counteract GOR A3G, the electrostatic interaction between these domains
282 may be crucial for the functional interaction between Vif and GOR A3G.
283
284 Surprisingly, the amino acid residue responsible for the counteraction of
285 GOR A3G was located in the Vif DRMR motif, which is required for degradation of
286 HU A3D and A3F (Russell et al., 2009; Sato et al., 2014). Additionally, the Vif
287 DRMR motif was less conserved in SIVgor and related HIV-1 (groups O and P),
288 while this motif was highly conserved in SIVcpz*Ptt* and related HIV-1 (groups M and
289 N). Moreover, the phylogenetic tree of the Vif DRMR motif revealed that SIVgor
290 forms a cluster with HIV-1 groups O and P. These findings indicated that the Vif
291 DRMR motif, in particular, has been lost when GOR was the host species. In this
292 regard, we demonstrated that the antiviral activity of GOR A3D and A3F is relatively
293 weaker than that of HU and CPZ counterparts. Taken together with these findings,
294 the skewed evolution of the Vif DRMR motif in GOR might be permitted due to the
295 selection pressure mediated by A3D and A3F being relaxed in GOR. Furthermore,
296 although the *vif* nucleotide sequence similarity between SIVcpz*Ptt* and SIVcpz*Pts*,
297 which is classified as the outgroup of HIV-1, SIVcpz*Ptt* and SIVgor, was relatively
298 low (p-distance between SIVcpz*Ptt* *vif* and SIVcpz*Pts* *vif* = 0.347 ± 0.016), the
299 DRMR motif is highly conserved in SIVcpz*Pts* and the phylogenetic tree of the Vif
300 DRMR motif indicated that SIVcpz*Pts* forms a cluster with SIVcpz*Ptt* and related
301 HIV-1s. These observations further suggest that the loss of the Vif DRMR motif may
302 be specific to SIVgor and related viruses.

bioRxiv preprint doi: https://doi.org/10.1101/362079; this version posted July 4, 2018. The copyright holder for this preprint (which was not certified by peer review) is the author/funder, who has granted bioRxiv a license to display the preprint in perpetuity. It is made available under aCC-BY-NC-ND 4.0 International license.

303

304 Although SIVgor and related HIV-1s lost the Vif DRMR motif in GOR,
305 these Vifs showed the ability to counteract A3D and A3F from GOR and HU. These
306 findings suggest that the loss of the DRMR motif resulted in the acquisition of novel
307 domain(s) to counteract A3D and A3F and to maintain Vif's integrity. In addition to
308 the distorted evolution in the Vif DRMR motif, previous studies suggested that other
309 viral antagonists, Vpu and Nef, have uniquely evolved in GOR: based on the
310 findings that HIV-1M Vpu but not SIVcpz*Ptt* Vpu counteracts HU tetherin (Sauter et
311 al., 2009), it is implied that gain of anti-HU tetherin activity by Vpu is important for
312 cross-species lentiviral transmission from CPZ to HU [reviewed in (Kirchhoff, 2010)].
313 However, Kluge et al. revealed that HIV-1O Nef but not Vpu has gained the ability to
314 counteract HU tetherin (Kluge et al., 2014). Since HIV-1O emerged from SIVgor
315 (D'arc et al., 2015), this is another example of the unique evolution of lentiviral
316 genes in GOR. Therefore, the unique lentiviral evolution in GOR including the
317 distortion of the Vif DRMR motif may contribute to the relatively lower prevalence of
318 HIV-1 groups O and P in the human population in comparison to pandemic HIV-1
319 group M.

320

321 In summary, here we shed light on the evolutionary interplay between
322 lentiviral Vif and host A3 in great apes and demonstrated that the interplay between
323 Vif and A3 in GOR has uniquely affected the evolutionary episode of great ape
324 lentiviruses. We elucidated how SIVcpz*Ptt* Vif overcame a species barrier mediated
325 by GOR A3G. This is the first report explaining how great ape lentiviral Vif
326 dismantled the hurdle mediated by new host A3 that potently impedes
327 cross-species transmission of great ape lentiviruses, which has naturally occurred
328 in Africa.

bioRxiv preprint doi: https://doi.org/10.1101/362079; this version posted July 4, 2018. The copyright holder for this preprint (which was not certified by peer review) is the author/funder, who has granted bioRxiv a license to display the preprint in perpetuity. It is made available under aCC-BY-NC-ND 4.0 International license.

329 **STAR*METHODS**
330 ● KEY RESOURCES TABLE
331 ● CONTACT FOR REAGENT AND RESOURCE SHARING
332 ● EXPERIMENTAL MODEL AND SUBJECT DETAILS
333 ○ Cells and Viruses
334 ● METHOD DETAILS
335 ○ Molecular Phylogenetic
336 ○ Expression Plasmids
337 ○ Western Blotting
338 ○ TZM-bl Reporter Assay for Virus Infectivity Quantification
339 ○ Multi-Round Virus Infection
340 ● QUANTIFICATION AND STATISTICAL ANALYSIS
341
342 **Supplemental Information**
343 Supplemental Information includes three figures five tables and can be found with
344 this article online.

bioRxiv preprint doi: https://doi.org/10.1101/362079; this version posted July 4, 2018. The copyright holder for this preprint (which was not certified by peer review) is the author/funder, who has granted bioRxiv a license to display the preprint in perpetuity. It is made available under aCC-BY-NC-ND 4.0 International license.

345 **Author Contributions**

346 Y.N., K.Y., A.S., R.K., H.A., N.M., Y.Konno, I.K., S.N. and G.J.-F. performed the
347 experiments and analyzed the data. J.I. and K.S. conducted phylogenetic analyses.
348 T.I., Y.Koyanagi and R.S.H. provided reagents. K.S. conceived and designed the
349 experiments. T.I., R.S.H. and K.S. wrote the manuscript.

350

351 **Acknowledgments**

352 We would like to thank Beatrice H. Hahn and Frederic Bibollet-Ruche (University of
353 Pennsylvania, USA) and Frank Kirchhoff and Daniel Sauter (Ulm University,
354 Germany) for kindly providing the IMCs of some HIV-1, SIVcpz*Ptt* and SIVgor, and
355 James L. Riley (University of Pennsylvania, USA) for sharing the CCR5-expressing
356 lentivirus vector. We also thank Kotubu Misawa for dedicated support.
357 This study was supported in part by AMED J-PRIDE 18fm0208006h0002 (to K.S.),
358 AMED Research on HIV/AIDS 18fk0410019h0001 (to K.S.) and 18fk0410014h0001
359 (to Y.Koyanagi), JST CREST (to K.S.), JSPS KAKENHI for Scientific Research B
360 (Generative Research Fields) 16KT0111 (to K.S.), Scientific Research B 18H02662
361 (to K.S.) and Scientific Research on Innovative Areas 16H06429 (to K.S),
362 16K21723 (to K.S.) and 17H05813 (to K.S.), Takeda Science Foundation (to K.S.),
363 Smoking Research Foundation (to K.S.), Mishima Kaiun Memorial Foundation (to
364 K.S.), Tobemaki Foundation (to K.S.), ONO Medical Research Foundation (to K.S.),
365 Joint Usage/Research Center program of Institute for Frontier Life and Medical
366 Sciences, Kyoto University (to K.S.), and JSPS Core-to-Core program, A.
367 Advanced Research Networks (to Y.Koyanagi, R.S.H. and K.S.), and NIAID R37
368 AI064046 (to R.S.H.). R.S.H. is the Margaret Harvey Schering Land Grant Chair for
369 Cancer Research, a Distinguished McKnight University Professor, and an
370 Investigator of the Howard Hughes Medical Institute.

bioRxiv preprint doi: https://doi.org/10.1101/362079; this version posted July 4, 2018. The copyright holder for this preprint (which was not certified by peer review) is the author/funder, who has granted bioRxiv a license to display the preprint in perpetuity. It is made available under aCC-BY-NC-ND 4.0 International license.

371 **References**

372 Barre-Sinoussi, F., Chermann, J.C., Rey, F., Nugeyre, M.T., Chamaret, S., Gruest,
373 J., Dauguet, C., Axler-Blin, C., Vezinet-Brun, F., Rouzioux, C., et al. (1983).
374 Isolation of a T-lymphotropic retrovirus from a patient at risk for acquired immune
375 deficiency syndrome (AIDS). Science *220*, 868-871.
376 Bibollet-Ruche, F., Heigele, A., Keele, B.F., Easlick, J.L., Decker, J.M., Takehisa, J.,
377 Learn, G., Sharp, P.M., Hahn, B.H., and Kirchhoff, F. (2012). Efficient SIVcpz
378 replication in human lymphoid tissue requires viral matrix protein adaptation. J Clin
379 Invest *122*, 1644-1652.
380 Compton, A.A., Bruel, T., Porrot, F., Mallet, A., Sachse, M., Euvrard, M., Liang, C.,
381 Casartelli, N., and Schwartz, O. (2014). IFITM proteins incorporated into HIV-1
382 virions impair viral fusion and spread. Cell Host Microbe *16*, 736-747.
383 Compton, A.A., and Emerman, M. (2013). Convergence and divergence in the
384 evolution of the APOBEC3G-Vif interaction reveal ancient origins of simian
385 immunodeficiency viruses. PLoS Pathog *9*, e1003135.
386 D'arc, M., Ayouba, A., Esteban, A., Learn, G.H., Boue, V., Liegeois, F., Etienne, L.,
387 Tagg, N., Leendertz, F.H., Boesch, C., et al. (2015). Origin of the HIV-1 group O
388 epidemic in western lowland gorillas. Proc Natl Acad Sci U S A *112*, E1343-1352.
389 Doyle, T., Goujon, C., and Malim, M.H. (2015). HIV-1 and interferons: who's
390 interfering with whom? Nat Rev Microbiol *13*, 403-413.
391 Gao, F., Bailes, E., Robertson, D.L., Chen, Y., Rodenburg, C.M., Michael, S.F.,
392 Cummins, L.B., Arthur, L.O., Peeters, M., Shaw, G.M., et al. (1999). Origin of HIV-1
393 in the chimpanzee Pan troglodytes troglodytes. Nature *397*, 436-441.
394 Harris, R.S., and Dudley, J.P. (2015). APOBECs and virus restriction. Virology
395 *479-480*, 131-145.
396 Keele, B.F., Van Heuverswyn, F., Li, Y., Bailes, E., Takehisa, J., Santiago, M.L.,
397 Bibollet-Ruche, F., Chen, Y., Wain, L.V., Liegeois, F., et al. (2006). Chimpanzee
398 reservoirs of pandemic and nonpandemic HIV-1. Science *313*, 523-526.
399 Kirchhoff, F. (2010). Immune evasion and counteraction of restriction factors by
400 HIV-1 and other primate lentiviruses. Cell Host Microbe *8*, 55-67.
401 Kluge, S.F., Mack, K., Iyer, S.S., Pujol, F.M., Heigele, A., Learn, G.H., Usmani, S.M.,
402 Sauter, D., Joas, S., Hotter, D., et al. (2014). Nef proteins of epidemic HIV-1 group
403 O strains antagonize human tetherin. Cell Host Microbe *16*, 639-650.
404 Kluge, S.F., Sauter, D., and Kirchhoff, F. (2015). SnapShot: antiviral restriction
405 factors. Cell *163*, 774-774 e771.
406 Kumar, S., Stecher, G., and Tamura, K. (2016). MEGA7: Molecular Evolutionary
407 Genetics Analysis Version 7.0 for Bigger Datasets. Mol Biol Evol *33*, 1870-1874.
408 Letko, M., Booiman, T., Kootstra, N., Simon, V., and Ooms, M. (2015). Identification

bioRxiv preprint doi: https://doi.org/10.1101/362079; this version posted July 4, 2018. The copyright holder for this preprint (which was not certified by peer review) is the author/funder, who has granted bioRxiv a license to display the preprint in perpetuity. It is made available under aCC-BY-NC-ND 4.0 International license.

409 of the HIV-1 Vif and Human APOBEC3G Protein Interface. Cell Rep *13*, 1789-1799.
410 Letko, M., Silvestri, G., Hahn, B.H., Bibollet-Ruche, F., Gokcumen, O., Simon, V.,
411 and Ooms, M. (2013). Vif proteins from diverse primate lentiviral lineages use the
412 same binding site in APOBEC3G. J Virol *87*, 11861-11871.
413 Nakano, Y., Aso, H., Soper, A., Yamada, E., Moriwaki, M., Juarez-Fernandez, G.,
414 Koyanagi, Y., and Sato, K. (2017a). A conflict of interest: the evolutionary arms race
415 between mammalian APOBEC3 and lentiviral Vif. Retrovirology *14*, 31.
416 Nakano, Y., Misawa, N., Juarez-Fernandez, G., Moriwaki, M., Nakaoka, S., Funo,
417 T., Yamada, E., Soper, A., Yoshikawa, R., Ebrahimi, D., et al. (2017b). HIV-1
418 competition experiments in humanized mice show that APOBEC3H imposes
419 selective pressure and promotes virus adaptation. PLoS Pathog *13*, e1006348.
420 Neil, S.J., Zang, T., and Bieniasz, P.D. (2008). Tetherin inhibits retrovirus release
421 and is antagonized by HIV-1 Vpu. Nature *451*, 425-430.
422 Parry, R.V., Rumbley, C.A., Vandenberghe, L.H., June, C.H., and Riley, J.L. (2003).
423 CD28 and inducible costimulatory protein Src homology 2 binding domains show
424 distinct regulation of phosphatidylinositol 3-kinase, Bcl-xL, and IL-2 expression in
425 primary human CD4 T lymphocytes. J Immunol *171*, 166-174.
426 Refsland, E.W., Stenglein, M.D., Shindo, K., Albin, J.S., Brown, W.L., and Harris,
427 R.S. (2010). Quantitative profiling of the full APOBEC3 mRNA repertoire in
428 lymphocytes and tissues: implications for HIV-1 restriction. Nucleic Acids Res *38*,
429 4274-4284.
430 Russell, R.A., Smith, J., Barr, R., Bhattacharyya, D., and Pathak, V.K. (2009).
431 Distinct domains within APOBEC3G and APOBEC3F interact with separate regions
432 of human immunodeficiency virus type 1 Vif. J Virol *83*, 1992-2003.
433 Sato, K., Misawa, N., Takeuchi, J.S., Kobayashi, T., Izumi, T., Aso, H., Nagaoka, S.,
434 Yamamoto, K., Kimura, I., Konno, Y., et al. (2018). Experimental adaptive evolution
435 of simian immunodeficiency virus SIVcpz to pandemic human immunodeficiency
436 virus type 1 by using a humanized mouse model. J Virol *92*, e01905.
437 Sato, K., Takeuchi, J.S., Misawa, N., Izumi, T., Kobayashi, T., Kimura, Y., Iwami, S.,
438 Takaori-Kondo, A., Hu, W.S., Aihara, K., et al. (2014). APOBEC3D and APOBEC3F
439 potently promote HIV-1 diversification and evolution in humanized mouse model.
440 PLoS Pathog *10*, e1004453.
441 Sauter, D., Schindler, M., Specht, A., Landford, W.N., Munch, J., Kim, K.A., Votteler,
442 J., Schubert, U., Bibollet-Ruche, F., Keele, B.F., et al. (2009). Tetherin-driven
443 adaptation of Vpu and Nef function and the evolution of pandemic and
444 nonpandemic HIV-1 strains. Cell Host Microbe *6*, 409-421.
445 Sharp, P.M., and Hahn, B.H. (2011). Origins of HIV and the AIDS pandemic. Cold
446 Spring Harb Perspect Med *1*, a006841.

bioRxiv preprint doi: https://doi.org/10.1101/362079; this version posted July 4, 2018. The copyright holder for this preprint (which was not certified by peer review) is the author/funder, who has granted bioRxiv a license to display the preprint in perpetuity. It is made available under aCC-BY-NC-ND 4.0 International license.

447 Takehisa, J., Kraus, M.H., Ayouba, A., Bailes, E., Van Heuverswyn, F., Decker,
448 J.M., Li, Y., Rudicell, R.S., Learn, G.H., Neel, C., et al. (2009). Origin and biology of
449 simian immunodeficiency virus in wild-living western gorillas. J Virol *83*, 1635-1648.
450 Van Damme, N., Goff, D., Katsura, C., Jorgenson, R.L., Mitchell, R., Johnson, M.C.,
451 Stephens, E.B., and Guatelli, J. (2008). The interferon-induced protein BST-2
452 restricts HIV-1 release and is downregulated from the cell surface by the viral Vpu
453 protein. Cell Host Microbe *3*, 245-252.
454 Van Heuverswyn, F., Li, Y., Neel, C., Bailes, E., Keele, B.F., Liu, W., Loul, S., Butel,
455 C., Liegeois, F., Bienvenue, Y., et al. (2006). Human immunodeficiency viruses: SIV
456 infection in wild gorillas. Nature *444*, 164.
457 Vanden Haesevelde, M.M., Peeters, M., Jannes, G., Janssens, W., van der Groen,
458 G., Sharp, P.M., and Saman, E. (1996). Sequence analysis of a highly divergent
459 HIV-1-related lentivirus isolated from a wild captured chimpanzee. Virology *221*,
460 346-350.
461 Wei, X., Decker, J.M., Liu, H., Zhang, Z., Arani, R.B., Kilby, J.M., Saag, M.S., Wu,
462 X., Shaw, G.M., and Kappes, J.C. (2002). Emergence of resistant human
463 immunodeficiency virus type 1 in patients receiving fusion inhibitor (T-20)
464 monotherapy. Antimicrob Agents Chemother *46*, 1896-1905.
465 Yamada, E., Nakaoka, S., Klein, L., Reith, E., Langer, S., Hopfensperger, K., Iwami,
466 S., Schreiber, G., Kirchhoff, F., Koyanagi, Y., et al. (2018). Human-Specific
467 Adaptations in Vpu Conferring Anti-tetherin Activity Are Critical for Efficient Early
468 HIV-1 Replication In Vivo. Cell Host Microbe *23*, 110-120 e117.
469 Zhang, Z., Gu, Q., de Manuel Montero, M., Bravo, I.G., Marques-Bonet, T.,
470 Haussinger, D., and Munk, C. (2017). Stably expressed APOBEC3H forms a barrier
471 for cross-species transmission of simian immunodeficiency virus of chimpanzee to
472 humans. PLoS Pathog *13*, e1006746.
473

bioRxiv preprint doi: https://doi.org/10.1101/362079; this version posted July 4, 2018. The copyright holder for this preprint (which was not certified by peer review) is the author/funder, who has granted bioRxiv a license to display the preprint in perpetuity. It is made available under aCC-BY-NC-ND 4.0 International license.

474 **Figure legends**

475 **Figure 1. Cross-species lentiviral transmission in great apes**

476 (A) Phylogenetic tree of the *vif* gene of great ape lentiviruses. The *vif* sequences
477 were extracted from Los Alamos HIV sequence database
478 (https://www.hiv.lanl.gov/components/sequence/HIV/search/search.html) and the
479 phylogenetic tree was constructed as described in **STAR*METHODS**. The
480 bootstrap values are indicated as follows: *, >50%; **, >80%. Scale bar indicates
481 0.05 nucleotide substitutions per site. An uncollapsed tree is shown in **Figure S1A**,
482 and the accession numbers of viral sequences are summarized in **Table S1**.
483 (B) Scheme of cross-species lentiviral transmission in great apes.
484 (C and D) Anti-HU A3G activity of primate lentiviral Vif. HEK293T cells were
485 co-transfected with pNL4-3Δ*vif* and the expression plasmids for HU A3G and
486 indicated Vif. Cells and supernatants were harvested at two days post-transfection
487 and were used for Western blotting (C) and TZM-bl assay (D).
488 (E and F) Counteracting ability of SIVcpz and SIVgor Vif against GOR A3G.
489 HEK293T cells were co-transfected with pNL4-3Δ*vif* and the expression plasmids
490 for GOR A3G and the Vif of indicated viral strain. Cells and supernatants were
491 harvested at two days post-transfection and were used for Western blotting (E) and
492 TZM-bl assay (F).
493 For Western blotting, the input of cell lysate was standardized to TUBA, and
494 representative results are shown. For TZM-bl assay, the percentage of the value
495 without HU A3G (D) and the raw value (relative infectivity) determined by TZM-bl
496 assay (F) are shown. The mean values of nine independent experiments ± SEM are
497 shown, and statistically significant differences ($P < 0.05$) versus "no Vif" are shown
498 by asterisks.
499 See also **Figure S1** and **Table S1**.
500

501 **Figure 2. Gain-of-function of SIVcpz*Ptt* Vif to counteract GOR A3G**

502 (A) Scheme of SIVcpz*Ptt* MB897 Vif derivatives used in this study. The amino acid
503 sequences of respective mutants are shown in **Figure S2A**.
504 (B-D) Determination of the amino acid residue of SIV Vif that is responsible to
505 counteract GOR A3G. HEK293T cells were co-transfected with pNL4-3Δ*vif* and the
506 expression plasmids for GOR A3G (10 or 50 ng; the plasmid amount was

bioRxiv preprint doi: https://doi.org/10.1101/362079; this version posted July 4, 2018. The copyright holder for this preprint (which was not certified by peer review) is the author/funder, who has granted bioRxiv a license to display the preprint in perpetuity. It is made available under aCC-BY-NC-ND 4.0 International license.

507 normalized by empty vector) and the indicated Vif derivatives. Cells and
508 supernatants were harvested at two days post-transfection and were used for
509 Western blotting and TZM-bl assay.
510 (E and F) Multi-round replication assay. The infectious viruses of SIVcpz*Ptt* MB897
511 WT, M16E and E2X (*vif* deleted) derivatives were prepared as described in
512 **STAR*METHODS** and were inoculated into parental SupT11-CCR5 cells or the
513 SupT11-CCR5 stably expressing GOR A3G (see also **Figure S2B**) at MOI 0.1. (E)
514 Culture supernatant was harvested per two days and the amount of infectious
515 viruses was measured by using TZM-bl cells. (F) Area under the curve (AUC) of
516 respective virus infection culture is shown.
517 (G) Importance of M16E substitution in other SIVcpz*Ptt* strains to counteract GOR
518 A3G.
519 (H) Importance of acidic residue at position 16 of SIVcpz*Ptt* to counteract GOR
520 A3G.
521 In (G) and (H), HEK293T cells were co-transfected with pNL4-3Δ*vif* and the
522 expression plasmids for GOR A3G and the indicated Vif strains and derivatives.
523 Cells and supernatants were harvested at two days post-transfection and were
524 used for Western blotting (left) and TZM-bl assay (right).
525 For Western blotting, the input of cell lysate was standardized to TUBA, and
526 representative results are shown. For TZM-bl assay, the percentage of the value
527 without GOR A3G is shown. The mean values of nine independent experiments ±
528 SEM are shown. Statistically significant differences ($P < 0.05$) versus “CP2139”
529 (B-D, G and H) or “M16E” (E and F) are shown by red asterisks. NS, no statistical
530 significance.
531 See also **Figure S2**.
532

533 **Figure 3. Poor antiviral activity of GOR A3D and A3F**

534 Antiviral activity of great ape A3D (A and B) and A3F (C and D). HEK293T cells
535 were co-transfected with pNL4-3Δ*vif* and the different amounts of expression
536 plasmids for great ape A3D and A3F (0, 50, 100, and 200 ng; the plasmid amount
537 was normalized by empty vector). Cells and supernatants were harvested at two
538 days post-transfection and were used for Western blotting (A and C) and TZM-bl
539 assay (B and D). For Western blotting, the input of cell lysate was standardized to
540 TUBA, and representative results are shown. For TZM-bl assay, the infectivity value
541 without A3 was set to 100%.
542

bioRxiv preprint doi: https://doi.org/10.1101/362079; this version posted July 4, 2018. The copyright holder for this preprint (which was not certified by peer review) is the author/funder, who has granted bioRxiv a license to display the preprint in perpetuity. It is made available under aCC-BY-NC-ND 4.0 International license.

543 **Figure 4. Degradation of antiviral human A3D and A3F by HIV-1OP and**
544 **SIVgor Vif independently of DRMR motif**
545 (A) Relaxed selection in DRMR motif of SIVgor and related HIV-1 groups. Logo plot
546 of DRMR and YRHHY motifs in HIV-1MNOP, SIVcpz and SIVgor are shown. The
547 number in parenthesis (n) indicates the number of viral sequences used in this
548 analysis.
549 (B and C) Activity of primate lentiviral Vif against HU A3D and A3F. HEK293T cells
550 were co-transfected with pNL4-3Δ*vif* and the expression plasmids for HU A3 and
551 indicated Vif. Cells and supernatants were harvested at two days post-transfection
552 and were used for Western blotting (top) and TZM-bl assay (bottom).
553 (D) Scheme of HIV-1M JRCSF Vif derivatives used in this study.
554 (E and F) Vif's activity against HU A3D and A3F. HEK293T cells were
555 co-transfected with pNL4-3Δ*vif* and the expression plasmids for HU A3D (E) or A3F
556 (F) and indicated Vif. Cells and supernatants were harvested at two days
557 post-transfection and were used for Western blotting (left) and TZM-bl assay (right).
558 For Western blotting, the input of cell lysate was standardized to TUBA, and
559 representative results are shown. For TZM-bl assay, the percentage of the value
560 without HU A3 is shown. The mean values of six independent experiments ± SEM
561 are shown, and statistically significant differences ($P < 0.05$) versus "no Vif" are
562 shown by asterisks.
563 See also **Figure S3**.

bioRxiv preprint doi: https://doi.org/10.1101/362079; this version posted July 4, 2018. The copyright holder for this preprint (which was not certified by peer review) is the author/funder, who has granted bioRxiv a license to display the preprint in perpetuity. It is made available under aCC-BY-NC-ND 4.0 International license.

564 **STAR*METHODS**

565 **CONTACT FOR REAGENT AND RESOURSE SHARING**

566 Further information and requests for resources and reagents may be directed to
567 and will be fulfilled by the Lead Contact, Kei Sato (ksato@ims.u-tokyo.ac.jp).

568

569 **EXPERIMENTAL MODEL AND SUBJECT DETAILS**

570 **Cells and Viruses**

571 HEK293T cells (a human embryonic kidney cell line; ATCC CRL-1573) and TZM-bl
572 cells (obtained through the NIH AIDS Research and Reference Reagent Program)
573 (Wei et al., 2002) were maintained in Dulbecco's modified Eagle's medium (Sigma)
574 containing FCS and antibiotics. A T cell line SupT11 was prepared as reported
575 previously (Refsland et al., 2010). To create the SupT11 cells stably expressing
576 CCR5 (SupT11-CCR5), the CCR5-expressing lentivirus vector (Parry et al., 2003)
577 and used for transduction. A single cell subclone of SupT11-CCR5 was isolated by
578 limiting dilution. Surface expression levels of CD4, CCR5 and CXCR4 on
579 SupT11-CCR5 cells were analyzed by staining with anti-CD4-FITC (Miltenyi
580 Biotech; clone M-T466) or CD4-PE (Miltenyi Biotech; clone M-T466), CCR5-FITC
581 (BD Pharmingen; clone 2D7) and CXCR4-PE (BD Pharmingen; clone 12G5)
582 antibodies. To prepare the SupT11-CCR5 cells stably expressing GOR A3G
583 (SupT11-CCR5-GOR A3G), a GOR A3G expression plasmid was transfected into
584 SupT11-CCR5 cells using the Neon Transfection system (Thermo Fisher Scientific).
585 The transfected cells were selected with Puromycin (InvivoGen; 0.5 ng/ml) and the
586 expression of GOR A3G in the selected cell clone was analyzed by Western blotting
587 using anti-HU A3G antibody (**Figure S2C**). Parental SupT11-CCR5 and
588 SupT11-CCR5-GOR A3G cells were maintained in RPMI1640 (Sigma) containing
589 FCS and antibiotics.

590 HEK293T cells were transfected using PEI Max (Polysciences) according
591 to the manufacturer's protocol. Basically, the expression plasmids for flag-tagged
592 great ape A3D (HU, 50 ng; GOR, 200 ng), A3F (HU, 50 ng; GOR, 200 ng) or A3G
593 (HU, 10 ng; GOR, 50 ng) were co-transfected with pNL4-3Δ*vif* (500 ng), an
594 infectious molecular clone (IMC) of *vif*-deleted HIV-1M strain NL4-3 (Sato et al.,
595 2014), and HA-tagged Vif expression plasmid (500 ng) into HEK293T cells. At two
596 days post-transfection, the culture supernatants and transfected cells were

bioRxiv preprint doi: https://doi.org/10.1101/362079; this version posted July 4, 2018. The copyright holder for this preprint (which was not certified by peer review) is the author/funder, who has granted bioRxiv a license to display the preprint in perpetuity. It is made available under aCC-BY-NC-ND 4.0 International license.

597 harvested and were respectively used for TZM-bl assay and Western blotting as
598 described below. For the preparation of infectious viruses, the IMCs (1,000 ng)
599 were transfected into HEK293T cells. At two days post-transfection, the culture
600 supernatants were harvested, centrifuged, and then filtered through a
601 0.45-μm-pore-size filter. To titrate virus infectivity, TZM-bl assay was performed as
602 described below.
603

604 **METHOD DETAILS**

605 **Molecular Phylogenetic**

606 The *vif* open reading frame (ORF) sequences (listed in **Table S1**) were extracted
607 from Los Alamos National Laboratory HIV sequence database
608 (https://www.hiv.lanl.gov/components/sequence/HIV/search/search.html) and
609 aligned by using Clustal W implemented in MEGA 7 software (Kumar et al., 2016).
610 Maximum-likelihood phylogenetic trees (**Figures 1A, S1A and S3A**) were
611 constructed using MEGA 7 software (Kumar et al., 2016). The logoplot of Vif amino
612 acid sequence is constructed using WebLogo 3 (http://weblogo.threeplusone.com)
613 and the residues at positions 14-17 (DRMR motif) and 40-44 (YRHHY motif) are
614 shown in **Figure 4A**.
615

616 **Expression Plasmids**

617 To construct the expression plasmids for flag-tagged great ape A3s, pcDNA3.1
618 plasmid (Thermo Fisher Scientific) was used as a backbone. The expression
619 plasmids for flag-tagged HU A3D, A3F and A3G were used in our previous study
620 (Nakano et al., 2017b). To construct the expression plasmids for flag-tagged CPZ
621 and GOR A3s, the ORFs of CPZ A3D (JN247642), CPZ A3F (XM_525658), CPZ
622 A3G (NM_001009001), GOR A3D (JN247649), GOR A3F (JN247640) and GOR
623 A3G (AY639868) were synthesized by the GeneArt gene synthesis service (Thermo
624 Fisher Scientific). The obtained DNA fragments were inserted into EcoRV-NotI (for
625 A3D and A3F) or EcoRI-XhoI (for A3G) sites of pcDNA3.1 plasmid (Thermo Fisher
626 Scientific). To construct the expression plasmids for HA-tagged lentiviral Vifs,
627 pDON-AI plasmid (Takara) was used as a backbone. The expression plasmid for
628 the HA-tagged Vifs of HIV-1M NL4-3 (M19921), SIVcpz*Ptt* MB897 (JN835461) and
629 SIVcpz*Ptt* MT145 (JN835462) were used in our previous study (Sato et al., 2018).

bioRxiv preprint doi: https://doi.org/10.1101/362079; this version posted July 4, 2018. The copyright holder for this preprint (which was not certified by peer review) is the author/funder, who has granted bioRxiv a license to display the preprint in perpetuity. It is made available under aCC-BY-NC-ND 4.0 International license.

630 The HA-tagged Vif ORFs of HIV-1M JRCSF (M38429), HIV-1N DJO0131
631 (AY532635), HIV-1O BCF183, HIV-1O RBF206, HIV-1P RBF168 and SIVgor
632 CP2139 (FJ424866) were prepared by PCR using their IMCs as the templates and
633 primers listed in **Table S2**. The HA-tagged Vif ORFs of HIV-1P U14788
634 (HQ179987), SIVcpz*Ptt* CAM3 (AF115393), SIVcpz*Ptt* DP943 (EF535993),
635 SIVcpz*Ptt* LB7 (DQ373064), SIVgor CP684 (FJ424871) and SIVgor BPID2
636 (KP004994) were synthesized by the GeneArt gene synthesis service (Thermo
637 Fisher Scientific). The obtained DNA fragments were inserted into BamHI-SalI site
638 of pDON-AI plasmid (Takara). The Vif mutants of SIVcpz*Ptt* MB897 and other
639 strains were prepared by the GeneArt site-directed mutagenesis system (Thermo
640 Fisher Scientific) using the primers listed in **Table S3**. The expression plasmid for
641 HA-tagged JRCSF Vif derivatives (**Figure 4D**) were prepared by PCR using their
642 IMCs as the templates and primers listed in **Table S4**. The IMCs of SIVcpz*Ptt*
643 MB897 derivatives, M16E and E2X (*vif*-deleted) were generated by
644 mutagenesis/overlap extension PCR using the primers listed in **Table S5**.
645 Nucleotide sequences were determined by a DNA sequencing service (Fasmac),
646 and the sequence data were analyzed by Sequencher v5.1 software (Gene Codes
647 Corporation).
648

649 **Western Blotting**

650 Western blotting was performed as previously described (Nakano et al., 2017b;
651 Yamada et al., 2018) using the following antibodies: anti-HA (clone 3F10; Roche),
652 anti-Flag (clone M2; Sigma-Aldrich), anti-p24 goat antiserum (ViroStat),
653 anti-alpha-tubulin (TUBA; clone DM1A; Sigma-Aldrich); and anti-HU A3G rabbit
654 antiserum (NIH AIDS Reagent Program catalog number #10201). For Western
655 blotting of viral particles, 370 µl of viral supernatant was ultracentrifuged at 100,000
656 × g for 1 h at 4°C using a TL-100 instrument (Beckman), and the pellet was lysed
657 with 1 × SDS buffer. Transfected cells were lysed with RIPA buffer (25 mM HEPES
658 [pH 7.4], 50 mM NaCl, 1 mM $MgCl_2$, 50 µM $ZnCl_2$, 10% glycerol, 1% Triton X-100)
659 containing a protease inhibitor cocktail (Roche).
660

661 **TZM-bl Reporter Assay for Virus Infectivity Quantification**

662 TZM-bl assay was performed as previously described (Nakano et al., 2017b;

bioRxiv preprint doi: https://doi.org/10.1101/362079; this version posted July 4, 2018. The copyright holder for this preprint (which was not certified by peer review) is the author/funder, who has granted bioRxiv a license to display the preprint in perpetuity. It is made available under aCC-BY-NC-ND 4.0 International license.

663 Yamada et al., 2018). Briefly, 10 μl of virus supernatant was inoculated into TZM-bl
664 cells in 96-well plate (Nunc), and the β-galactosidase activity was measured by
665 using the Galacto-Star mammalian reporter gene assay system (Thermo Fisher
666 Scientific) and a 2030 ARVO X multi-label counter instrument (PerkinElmer)
667 according to the manufacturers' procedure. The relative infectivity was determined
668 by relative light unit of this assay.
669

670 **Multi-Round Virus Infection**

671 The virus supernatant of SIVcpz*Ptt* MB897 WT, M16E and E2X (*vif*-deleted)
672 derivatives were inoculated into SupT11-CCR5 (parental) and SupT11-CCR5-GOR
673 A3G cells at multiplicity of infection (MOI) 0.1. The culture supernatant was
674 harvested every two days and the amount of infectious viruses was measured by
675 TZM-bl assay.
676

677 **QUANTIFICATION AND STATISTICAL ANALYSIS**

678 Data analyses were performed using GraphPad Prism software. The data are
679 presented as averages ± SEM. Statistically significant differences were determined
680 by Student's *t* test. Statistical details can be found directly in the figures or in the
681 corresponding figure legends.

bioRxiv preprint doi: https://doi.org/10.1101/362079; this version posted July 4, 2018. The copyright holder for this preprint (which was not certified by peer review) is the author/funder, who has granted bioRxiv a license to display the preprint in perpetuity. It is made available under aCC-BY-NC-ND 4.0 International license.

STAR★METHODS

KEY RESOURCES TABLE

REAGENT or RESOURCE	SOURCE	IDENTIFIER
Antibodies		
HRP-conjugated anti-HA	Roche	Cat# 12013819001
HRP-conjugated anti-Flag	Sigma-Aldrich	Cat# A8592
Anti-HIV-1 p24	ViroStat	Cat# 1951
Anti-alpha-Tubulin	Sigma-Aldrich	Cat# T9026
Anti-HU A3G	NIH AIDS Reagent Program	Cat# 10201
FITC-conjugated anti-CD4	Miltenyi Biotech	Cat# 130-080-501
PE-conjugated anti-CD4	Miltenyi Biotech	Cat# 130-091-231
FITC-conjugated anti-CCR5	BD Biosciences	Cat# 555992
PE-conjugated anti-CXCR4	BD Biosciences	Cat# 555974
Bacterial and Virus Strains		
HIV-1 group M, strain NL4-3	(Adachi et al., 1986)	Genbank accession no. M19921
HIV-1 group M, strain JRCSF	(Koyanagi et al., 1987)	Genbank accession no. M38429
HIV-1 group M, strain NLCSFV3	(Suzuki et al., 1999)	N/A
HIV-1 group M, strain IIIBC200	(Hache et al., 2008; Ikeda et al., 2018)	N/A
HIV-1 group N, strain DJO0131	(Sauter et al., 2012)	Genbank accession no. AY532635
HIV-1 group O, strain BCF183	Not applicable	N/A
HIV-1 group O, strain RBF206	(Mack et al., 2017)	N/A
HIV-1 group P, strain RBF168	Not applicable	N/A
HIV-1 group P, strain U14788	(Vallari et al., 2011)	Genbank accession no. HQ179987
SIVcpz*Ptt*, strain MB897	(Bibollet-Ruche et al., 2012)	Genbank accession no. JN835461
SIVcpz*Ptt*, strain CAM3	(Corbet et al., 2000)	Genbank accession no. AF115393
SIVcpz*Ptt*, strain DP943	(Van Heuverswyn et al., 2007)	Genbank accession no. EF535993
SIVcpz*Ptt*, strain LB7	(Keele et al., 2006)	Genbank accession no. DQ373064
SIVcpz*Ptt*, strain MT145	(Bibollet-Ruche et al., 2012)	Genbank accession no. JN835462
SIVgor, strain CP2139	(Takehisa et al., 2009)	Genbank accession no. FJ424866
SIVgor, strain CP684	(Takehisa et al., 2009)	Genbank accession no. FJ424871
SIVgor, strain BPID2	(D'arc et al., 2015)	Genbank accession no. KP004994
Chemicals, Peptides, and Recombinant Proteins		

bioRxiv preprint doi: https://doi.org/10.1101/362079; this version posted July 4, 2018. The copyright holder for this preprint (which was not certified by peer review) is the author/funder, who has granted bioRxiv a license to display the preprint in perpetuity. It is made available under aCC-BY-NC-ND 4.0 International license.

PEI Max	Polysciences	Cat# 24765-1
L-glutamate	Thermo Fisher Scientific	Cat# 25030081
Puromycin	InvivoGen	Cat# ant-pr-5
PrimeSTAR GXL DNA polymerase	Takara	Cat# R050A
EcoRV	Takara	Cat# 1042A
NotI	Takara	Cat# 1166A
EcoRI	Takara	Cat# 1040A
XhoI	Takara	Cat# 1094A
BamHI	Takara	Cat# 1010A
SalI	Takara	Cat# 1080A
Critical Commercial Assays		
Galacto-Star mammalian reporter gene assay system	Thermo Fisher Scientific	Cat# T1014
Experimental Models: Cell Lines		
Human: HEK293T cells	ATCC	CRL-1573
Human: TZM-bl cells	NIH AIDS Reagent Program	Cat# 8129
Human: SupT11-CCR5 cells	This study	N/A
Human: SupT11-CCR5-GOR A3G cells	This study	N/A
Oligonucleotides		
Primers for construction of Vif expression plasmids, see **Table S2**	This study	N/A
Primers for construction of SIVcpz*Ptt* Vif derivatives, see **Table S3**	This study	N/A
Primers for construction of HIV-1M JRCSF Vif derivatives, see **Table S4**	This study	N/A
Primers for construction of SIVcpz*Ptt* MBV897 IMC derivatives, see **Table S5**	This study	N/A
Recombinant DNA		
Plasmid: pNL4-3Δ*vif* (IMC of *vif*-deleted HIV-1 group M strain NL4-3)	(Sato et al., 2014)	Genbank accession no. M19921
Plasmid: pJRCSF (HIV-1 group M strain JRCSF)	(Koyanagi et al., 1987)	Genbank accession no. M38429
Plasmid: pDJO0131 (HIV-1 group N strain DJO0131)	(Sauter et al., 2012)	Genbank accession no. AY532635
Plasmid: pBCF183 (HIV-1 group O strain BCF183)	Kindly provided by Daniel Sauter & Frank Kirchhoff	N/A

bioRxiv preprint doi: https://doi.org/10.1101/362079; this version posted July 4, 2018. The copyright holder for this preprint (which was not certified by peer review) is the author/funder, who has granted bioRxiv a license to display the preprint in perpetuity. It is made available under aCC-BY-NC-ND 4.0 International license.

Plasmid: pRBF206 (HIV-1 group O strain RBF206)	(Mack et al., 2017)	N/A
Plasmid: pRBF168 (HIV-1 group P strain RBF168)	Kindly provided by Beatrice Hahn & Frederic Bibollet-Ruche	N/A
Plasmid: pMB897 (IMC of SIVcpz*Ptt* MB897)	(Bibollet-Ruche et al., 2012)	Genbank accession no. JN835461
Plasmid: pMT145 (IMC of SIVcpz*Ptt* MT145)	(Bibollet-Ruche et al., 2012)	Genbank accession no. JN835462
Plasmid: pCP2139 (IMC of SIVgor CP2139)	(Takehisa et al., 2009)	Genbank accession no. FJ424866
Plasmid: pMB897 M16E (IMC of SIVcpz*Ptt* MB897 Vif M16E)	This study	N/A
Plasmid: pMB897 E2X (IMC of *vif*-deleted SIVcpz*Ptt* MB897)	This study	N/A
Plasmid: pcDNA3.1	Thermo Fisher Scientific	Cat# V800-20
Plasmid: pcDNA3.1 flag-tagged HU A3D	(Nakano et al., 2017)	N/A
Plasmid: pcDNA3.1 flag-tagged HU A3F	(Nakano et al., 2017)	N/A
Plasmid: pcDNA3.1 flag-tagged HU A3G	(Nakano et al., 2017)	N/A
Plasmid: pcDNA3.1 flag-tagged CPZ A3D	This study	Genbank accession no. JN247642
Plasmid: pcDNA3.1 flag-tagged CPZ A3F	This study	Genbank accession no. XM_525658
Plasmid: pcDNA3.1 flag-tagged CPZ A3G	This study	Genbank accession no. NM_001009001
Plasmid: pcDNA3.1 flag-tagged GOR A3D	This study	Genbank accession no. JN247649
Plasmid: pcDNA3.1 flag-tagged GOR A3F	This study	Genbank accession no. JN247640
Plasmid: pcDNA3.1 flag-tagged GOR A3G	This study	Genbank accession no. AY639868
Plasmid: pDON-AI	(Schubert et al., 1999; Schubert et al., 1995)Takara	N/A
Plasmid: pDON-AI HA-tagged NL4-3 Vif	(Nakano et al., 2017)	N/A
Plasmids: pDON-AI HA-tagged Vif expression plasmids, see **Table S2**	This study	N/A
Plasmids: pDON-AI HA-tagged SIVcpz*Ptt* Vif derivatives, see **Table S3**	This study	N/A
Plasmids: pDON-AI HA-tagged HIV-1M JRCSF Vif derivatives, see **Table S4**	This study	N/A
Software and Algorithms		
GraphPad Prism	GraphPad Software	https://www.graphpad.com/scientific-software/prism/

bioRxiv preprint doi: https://doi.org/10.1101/362079; this version posted July 4, 2018. The copyright holder for this preprint (which was not certified by peer review) is the author/funder, who has granted bioRxiv a license to display the preprint in perpetuity. It is made available under aCC-BY-NC-ND 4.0 International license.

MEGA 7	(Kumar et al., 2016)	https://www.megasoftware.net
Clustal W	(Thompson et al., 1994)	http://clustalw.ddbj.nig.ac.jp
Weblogo 3	N/A	http://weblogo.threeplusone.com
Los Alamos National Library HIV sequence database	N/A	https://www.hiv.lanl.gov/components/sequence/HIV/search/search.html
Other		
0.45-μm-pore-size filter	Merck Millipore	Cat# SLHV033RB

References

Adachi, A., Gendelman, H.E., Koenig, S., Folks, T., Willey, R., Rabson, A., and Martin, M.A. (1986). Production of acquired immunodeficiency syndrome-associated retrovirus in human and nonhuman cells transfected with an infectious molecular clone. J Virol *59*, 284-291.

Bibollet-Ruche, F., Heigele, A., Keele, B.F., Easlick, J.L., Decker, J.M., Takehisa, J., Learn, G., Sharp, P.M., Hahn, B.H., and Kirchhoff, F. (2012). Efficient SIVcpz replication in human lymphoid tissue requires viral matrix protein adaptation. J Clin Invest *122*, 1644-1652.

Corbet, S., Muller-Trutwin, M.C., Versmisse, P., Delarue, S., Ayouba, A., Lewis, J., Brunak, S., Martin, P., Brun-Vezinet, F., Simon, F., et al. (2000). env sequences of simian immunodeficiency viruses from chimpanzees in Cameroon are strongly related to those of human immunodeficiency virus group N from the same geographic area. J Virol *74*, 529-534.

D'arc, M., Ayouba, A., Esteban, A., Learn, G.H., Boue, V., Liegeois, F., Etienne, L., Tagg, N., Leendertz, F.H., Boesch, C., et al. (2015). Origin of the HIV-1 group O epidemic in western lowland gorillas. Proc Natl Acad Sci U S A *112*, E1343-1352.

Hache, G., Shindo, K., Albin, J.S., and Harris, R.S. (2008). Evolution of HIV-1 isolates that use a novel Vif-independent mechanism to resist restriction by human APOBEC3G. Curr Biol *18*, 819-824.

Ikeda, T., Symeonides, M., Albin, J.S., Li, M., Thali, M., and Harris, R.S. (2018). HIV-1 adaptation studies reveal a novel Env-mediated homeostasis mechanism for evading lethal hypermutation by APOBEC3G. PLoS Pathog *14*, e1007010.

Keele, B.F., Van Heuverswyn, F., Li, Y., Bailes, E., Takehisa, J., Santiago, M.L., Bibollet-Ruche, F., Chen, Y., Wain, L.V., Liegeois, F., et al. (2006). Chimpanzee reservoirs of pandemic and nonpandemic HIV-1. Science *313*, 523-526.

Koyanagi, Y., Miles, S., Mitsuyasu, R.T., Merrill, J.E., Vinters, H.V., and Chen, I.S. (1987). Dual infection of the central nervous system by AIDS viruses with distinct cellular tropisms. Science *236*, 819-822.

Kumar, S., Stecher, G., and Tamura, K. (2016). MEGA7: Molecular Evolutionary Genetics Analysis Version 7.0 for Bigger Datasets. Mol Biol Evol *33*, 1870-1874.

Mack, K., Starz, K., Sauter, D., Langer, S., Bibollet-Ruche, F., Learn, G.H., Sturzel, C.M., Leoz, M., Plantier, J.C., Geyer, M., et al. (2017). Efficient Vpu-Mediated Tetherin Antagonism by an

bioRxiv preprint doi: https://doi.org/10.1101/362079; this version posted July 4, 2018. The copyright holder for this preprint (which was not certified by peer review) is the author/funder, who has granted bioRxiv a license to display the preprint in perpetuity. It is made available under aCC-BY-NC-ND 4.0 International license.

HIV-1 Group O Strain. J Virol *91*.

Nakano, Y., Misawa, N., Juarez-Fernandez, G., Moriwaki, M., Nakaoka, S., Funo, T., Yamada, E., Soper, A., Yoshikawa, R., Ebrahimi, D., et al. (2017). HIV-1 competition experiments in humanized mice show that APOBEC3H imposes selective pressure and promotes virus adaptation. PLoS Pathog *13*, e1006348.

Sato, K., Takeuchi, J.S., Misawa, N., Izumi, T., Kobayashi, T., Kimura, Y., Iwami, S., Takaori-Kondo, A., Hu, W.S., Aihara, K., et al. (2014). APOBEC3D and APOBEC3F potently promote HIV-1 diversification and evolution in humanized mouse model. PLoS Pathog *10*, e1004453.

Sauter, D., Unterweger, D., Vogl, M., Usmani, S.M., Heigele, A., Kluge, S.F., Hermkes, E., Moll, M., Barker, E., Peeters, M., et al. (2012). Human tetherin exerts strong selection pressure on the HIV-1 group N Vpu protein. PLoS Pathog *8*, e1003093.

Schubert, U., Bour, S., Willey, R.L., and Strebel, K. (1999). Regulation of virus release by the macrophage-tropic human immunodeficiency virus type 1 AD8 isolate is redundant and can be controlled by either Vpu or Env. J Virol *73*, 887-896.

Schubert, U., Clouse, K.A., and Strebel, K. (1995). Augmentation of virus secretion by the human immunodeficiency virus type 1 Vpu protein is cell type independent and occurs in cultured human primary macrophages and lymphocytes. J Virol *69*, 7699-7711.

Suzuki, Y., Koyanagi, Y., Tanaka, Y., Murakami, T., Misawa, N., Maeda, N., Kimura, T., Shida, H., Hoxie, J.A., O'Brien, W.A., et al. (1999). Determinant in human immunodeficiency virus type 1 for efficient replication under cytokine-induced CD4+ T-helper 1 (Th1)- and Th2-type conditions. J Virol *73*, 316-324.

Takehisa, J., Kraus, M.H., Ayouba, A., Bailes, E., Van Heuverswyn, F., Decker, J.M., Li, Y., Rudicell, R.S., Learn, G.H., Neel, C., et al. (2009). Origin and biology of simian immunodeficiency virus in wild-living western gorillas. J Virol *83*, 1635-1648.

Thompson, J.D., Higgins, D.G., and Gibson, T.J. (1994). CLUSTAL W: improving the sensitivity of progressive multiple sequence alignment through sequence weighting, position-specific gap penalties and weight matrix choice. Nucleic Acids Res *22*, 4673-4680.

Vallari, A., Holzmayer, V., Harris, B., Yamaguchi, J., Ngansop, C., Makamche, F., Mbanya, D., Kaptue, L., Ndembi, N., Gurtler, L., et al. (2011). Confirmation of putative HIV-1 group P in Cameroon. J Virol *85*, 1403-1407.

Van Heuverswyn, F., Li, Y., Bailes, E., Neel, C., Lafay, B., Keele, B.F., Shaw, K.S., Takehisa, J., Kraus, M.H., Loul, S., et al. (2007). Genetic diversity and phylogeographic clustering of SIVcpz*Ptt* in wild chimpanzees in Cameroon. Virology *368*, 155-171.

A

HIV-1M
SIVcpz*Ptt*
SIVcpz*Ptt*
SIVcpz*Ptt*
HIV-1N
SIVcpz*Ptt*
SIVcpz*Ptt*
HIV-1P
SIVgor
SIVgor
SIVgor
SIVgor
HIV-1O
SIVcpz*Pts*
0.05

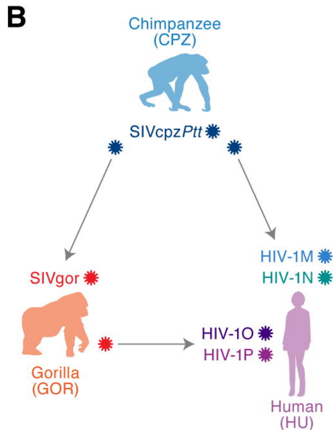

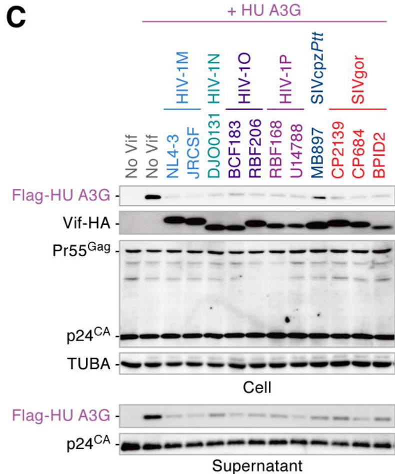

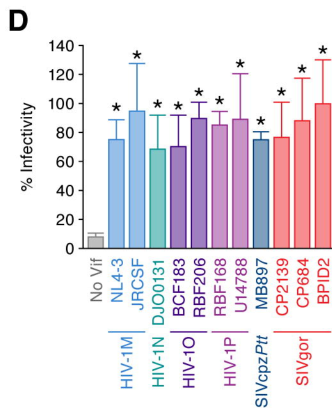

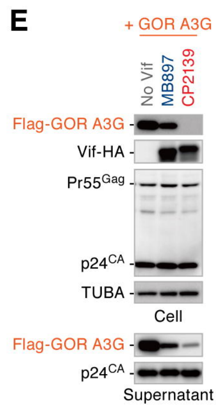

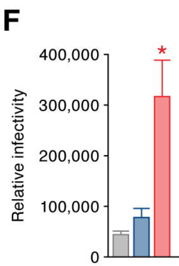

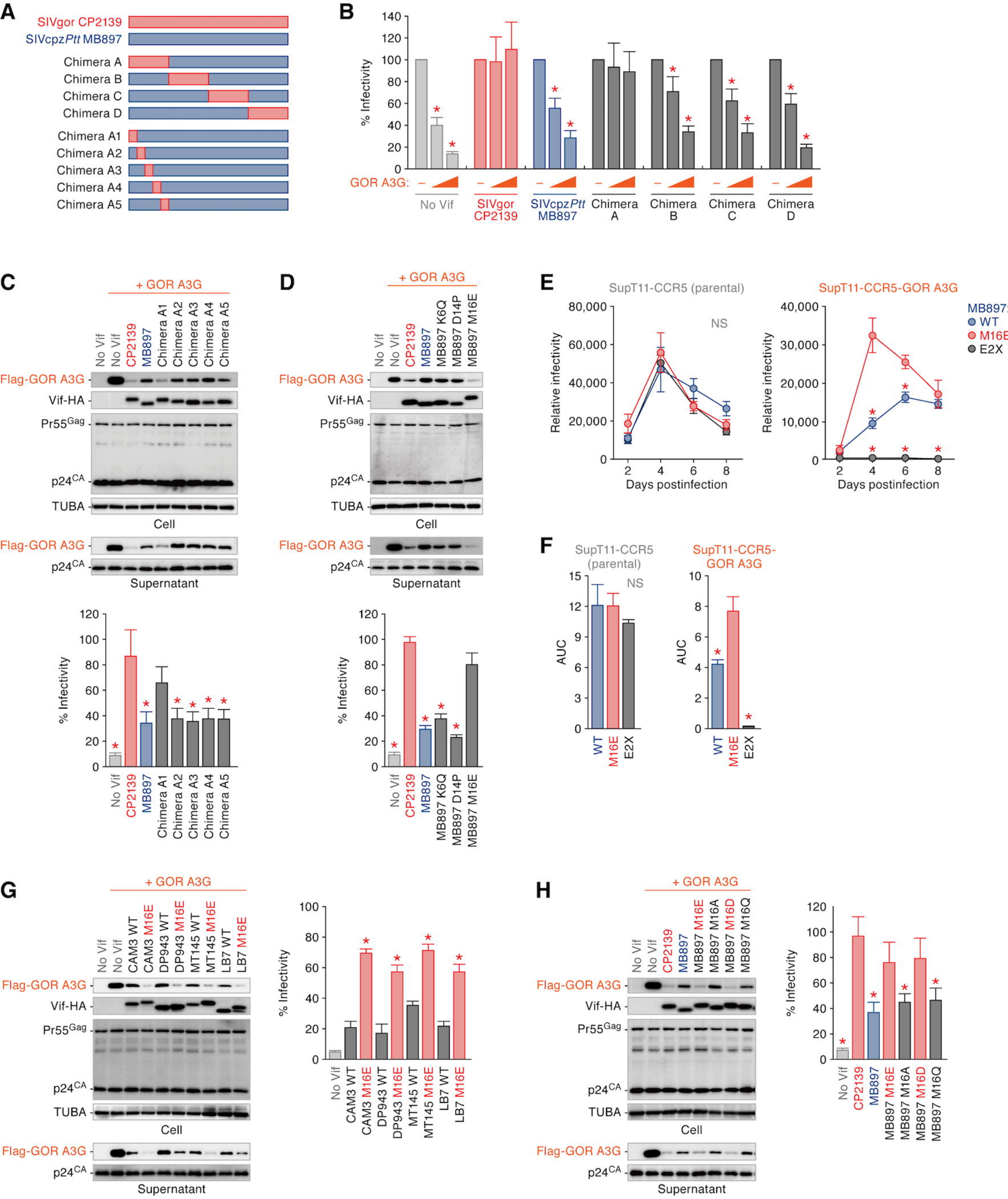

A
SIVgor CP2139
SIVcpzPtt MB897
Chimera A
Chimera B
Chimera C
Chimera D
Chimera A1
Chimera A2
Chimera A3
Chimera A4
Chimera A5
B
% Infectivity
GOR A3G:
No Vif
SIVgor CP2139
SIVcpzPtt MB897
Chimera A
Chimera B
Chimera C
Chimera D
C
+ GOR A3G
No Vif
No Vif
CP2139
MB897
Chimera A1
Chimera A2
Chimera A3
Chimera A4
Chimera A5
Flag-GOR A3G
Vif-HA
Pr55Gag
p24CA
TUBA
Cell
Flag-GOR A3G
p24CA
Supernatant
% Infectivity
D
+ GOR A3G
No Vif
No Vif
CP2139
MB897
MB897 K6Q
MB897 D14P
MB897 M16E
Flag-GOR A3G
Vif-HA
Pr55Gag
p24CA
TUBA
Cell
Flag-GOR A3G
p24CA
Supernatant
% Infectivity
E
SupT11-CCR5 (parental)
NS
Relative infectivity
Days postinfection
SupT11-CCR5-GOR A3G
Relative infectivity
Days postinfection
MB897:
WT
M16E
E2X
F
SupT11-CCR5 (parental)
NS
AUC
WT
M16E
E2X
SupT11-CCR5-GOR A3G
AUC
WT
M16E
E2X
G
+ GOR A3G
No Vif
No Vif
CAM3 WT
CAM3 M16E
DP943 WT
DP943 M16E
MT145 WT
MT145 M16E
LB7 WT
LB7 M16E
Flag-GOR A3G
Vif-HA
Pr55Gag
p24CA
TUBA
Cell
Flag-GOR A3G
p24CA
Supernatant
% Infectivity
H
+ GOR A3G
No Vif
No Vif
CP2139
MB897
MB897 M16E
MB897 M16A
MB897 M16D
MB897 M16Q
Flag-GOR A3G
Vif-HA
Pr55Gag
p24CA
TUBA
Cell
Flag-GOR A3G
p24CA
Supernatant
% Infectivity

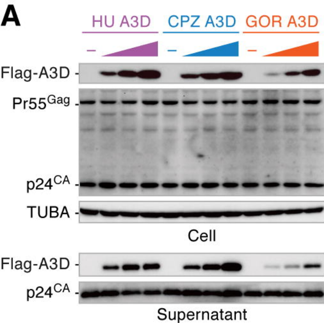
A
HU A3D
CPZ A3D
GOR A3D
Flag-A3D
Pr55^Gag
p24^CA
TUBA
Cell
Flag-A3D
p24^CA
Supernatant

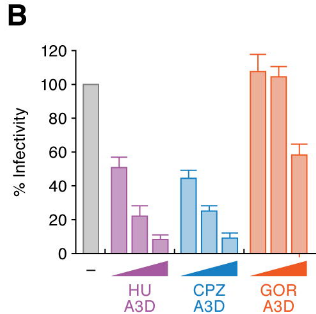
B
% Infectivity
120
100
80
60
40
20
0
HU A3D
CPZ A3D
GOR A3D

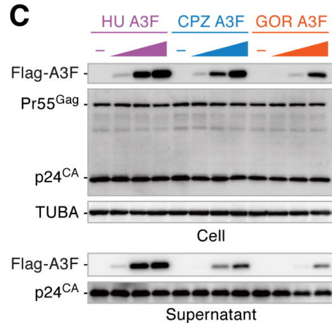
C
HU A3F
CPZ A3F
GOR A3F
Flag-A3F
Pr55^Gag
p24^CA
TUBA
Cell
Flag-A3F
p24^CA
Supernatant

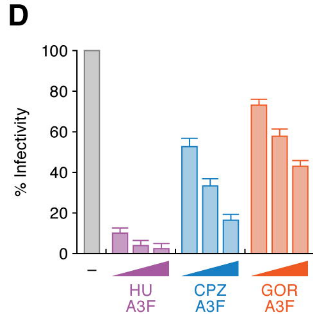
D
% Infectivity
100
80
60
40
20
0
HU A3F
CPZ A3F
GOR A3F

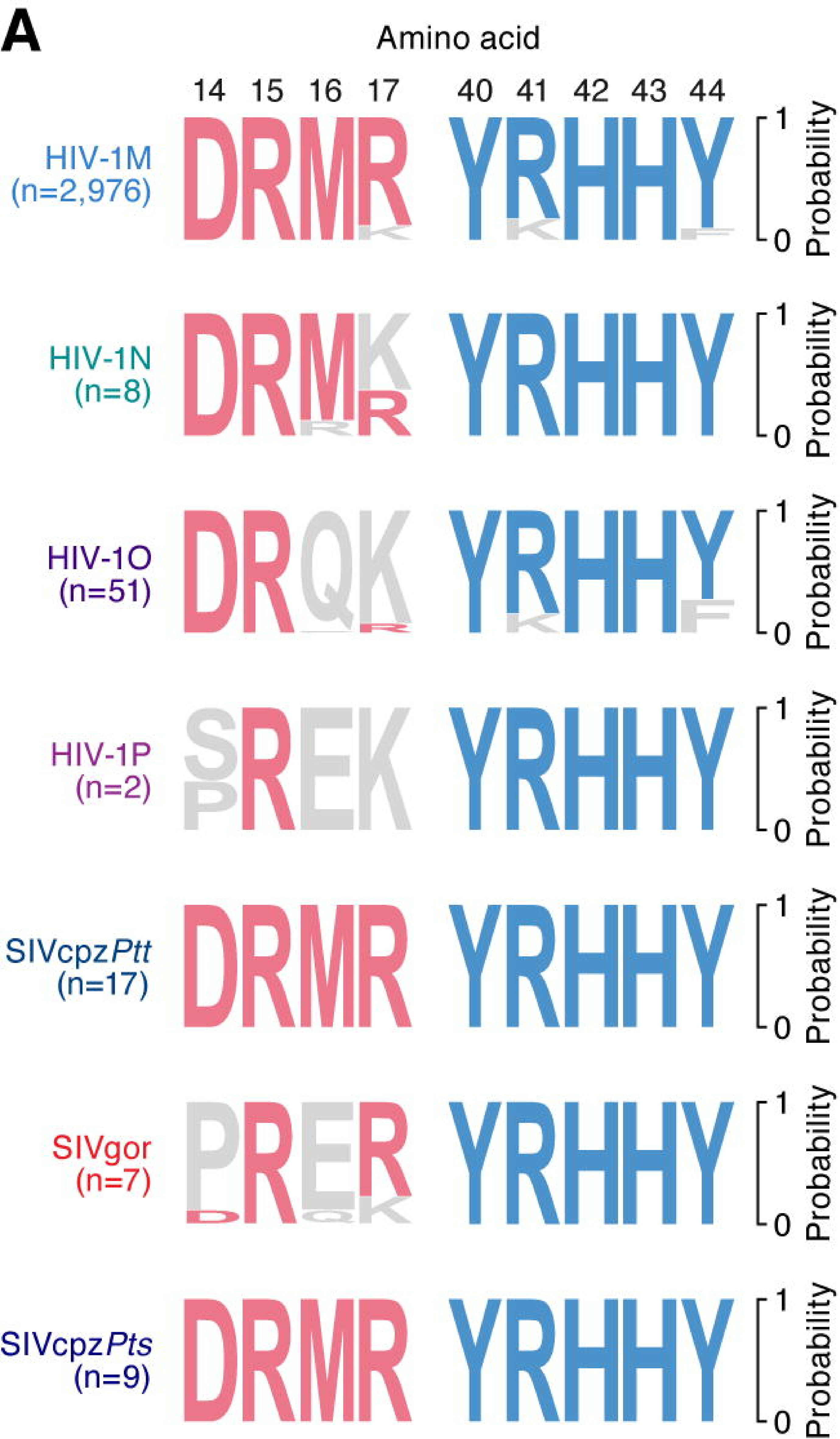

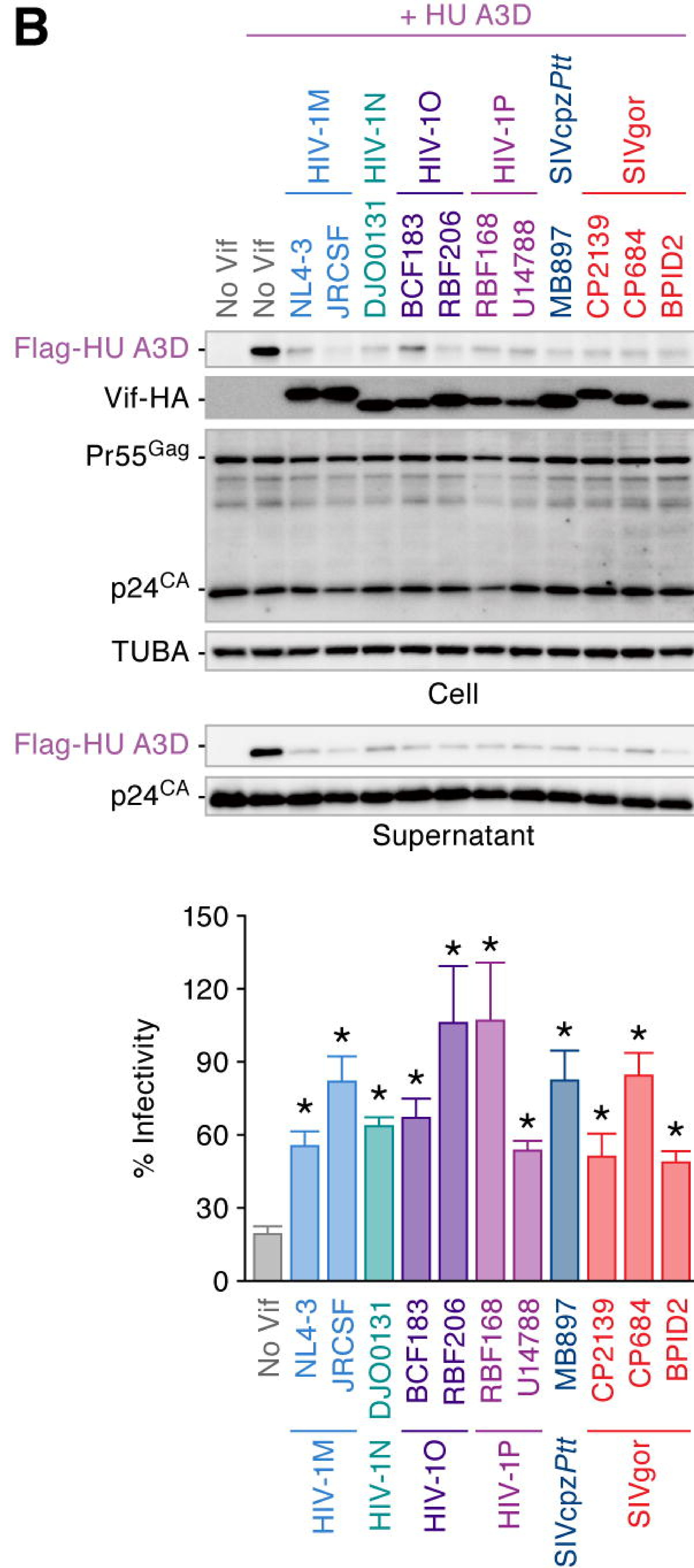

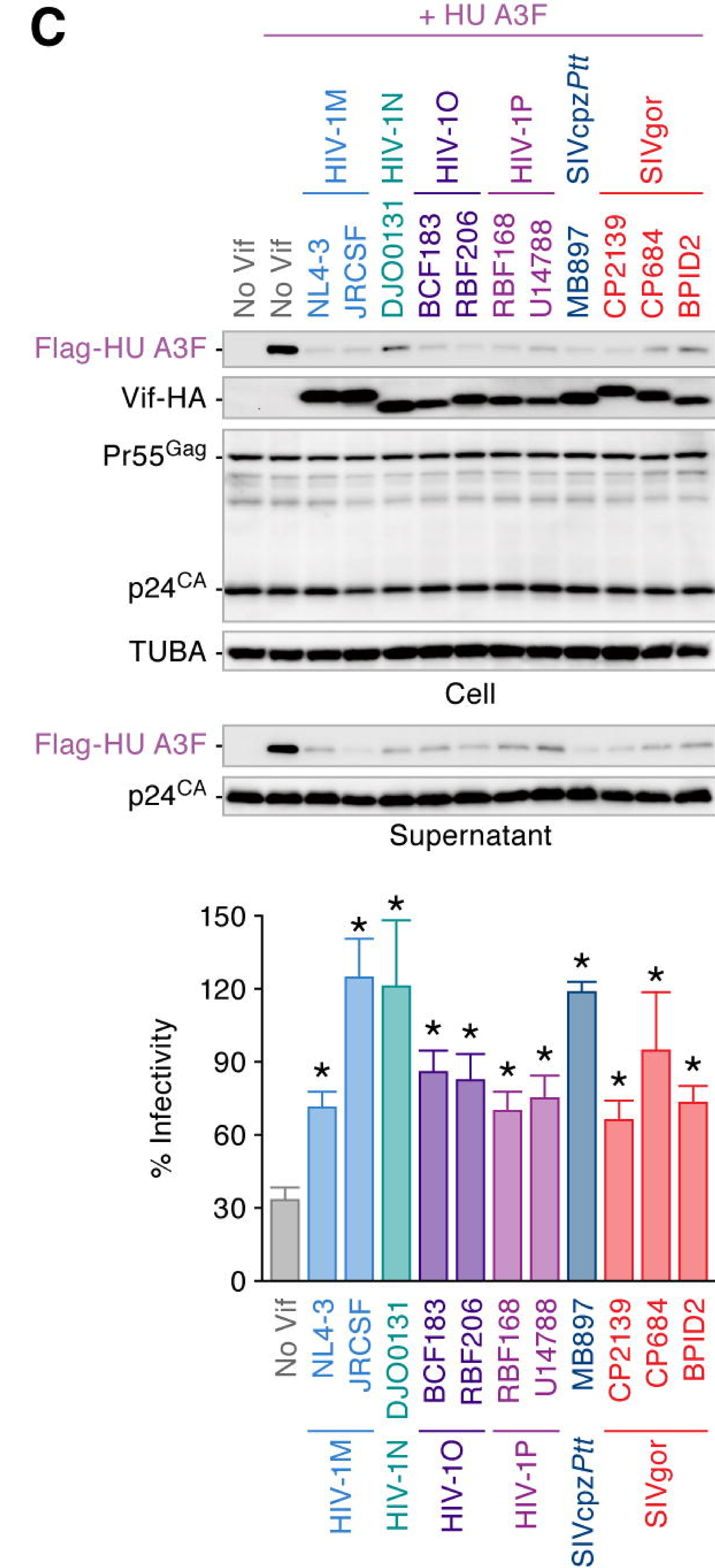

bioRxiv preprint doi: https://doi.org/10.1101/362079; this version posted July 4, 2018. The copyright holder for this preprint (which was not certified by peer review) is the author/funder, who has granted bioRxiv a license to display the preprint in perpetuity. It is made available under aCC-BY-NC-ND 4.0 International license.